RECENT DEVELOPMENT AND APPLICATIONS OF WENO SCHEMES

CHI-WANG SHU
Division of Applied Mathematics, Brown University
Providence, RI 02912, USA. E-mail: shu@cfm.brown.edu

Abstract. This paper is a summary of the author's talk given in the Third AFOSR International Conference on DNS/LES (TAICDL), held at the University of Texas at Arlington on August 5-9, 2001. In this paper we briefly present the general ideas of high order accurate weighted essentially non-oscillatory (WENO) schemes, and describe the similarities and differences of the two classes of WENO schemes: finite volume schemes and finite difference schemes. We also briefly mention two recent developments of WENO schemes, namely a technique to treat negative linear weights and a class of high order central WENO schemes.

1. Introduction

This paper is a summary of my talk given in the Third AFOSR International Conference on DNS/LES (TAICDL), held at the University of Texas at Arlington on August 5-9, 2001. In this paper we briefly present the general ideas of high order accurate weighted essentially non-oscillatory (WENO) schemes, and describe the similarities and differences of the two classes of WENO schemes: finite volume schemes and finite difference schemes. We also briefly mention two recent developments of WENO schemes, namely a technique to treat negative linear weights and a class of high order central WENO schemes.

High order accurate weighted essentially non-oscillatory (WENO) schemes have been developed to solve a hyperbolic conservation law

$$u_t + \nabla \cdot f(u) = 0. \tag{1.1}$$

The first WENO scheme was constructed in [19] for a third order finite volume version in one space dimension. In [11], third and fifth order finite dif-

ference WENO schemes in multiple space dimensions are constructed, with a general framework for the design of the smoothness indicators and nonlinear weights. Later, second, third and fourth order finite volume WENO schemes for 2D general triangulation have been developed in [5] and [9]. Very high order finite difference WENO schemes (for orders between 7 and 11) have been developed in [1]. Central WENO schemes have been developed in [13], [14], [15] and [22]. A technique to treat negative linear weights in WENO schemes has been developed in [23]. In this conference, Jiang, Shan and Liu presented their new results on developing compact WENO schemes.

WENO schemes are designed based on the successful ENO schemes in [8, 26, 27]. Both ENO and WENO schemes use the idea of adaptive stencils in the reconstruction procedure based on the local smoothness of the numerical solution to automatically achieve high order accuracy and non-oscillatory property near discontinuities. ENO uses just one (optimal in some sense) out of many candidate stencils when doing the reconstruction; while WENO uses a convex combination of all the candidate stencils, each being assigned a nonlinear weight which depends on the local smoothness of the numerical solution based on that stencil. WENO improves upon ENO in robustness, better smoothness of fluxes, better steady state convergence, better provable convergence properties, and more efficiency. For a detailed review of ENO and WENO schemes, up to the time when these notes were published, we refer to the lecture notes [24, 25].

WENO schemes have already been widely used in applications. Some of the examples include dynamical response of a stellar atmosphere to pressure perturbations [4]; shock vortex interactions and other gas dynamics problems [6], [7]; incompressible flow problems [28]; Hamilton-Jacobi equations [10]; magneto-hydrodynamics [12]; underwater blast-wave focusing [16]; the composite schemes and shallow water equations [17], [18], real gas computations [20], wave propagation using Fey's method of transport [21]; etc. In this conference and in this volume, we have seen several new developments and applications of WENO schemes for DNS/LES of turbulence flows.

The organization of this paper is as follows. In section 2 we discuss two different formulations of WENO schemes, namely the finite volume formulation and the finite difference formulation, and point out their similarities and differences, both in one dimension and in multiple space dimensions. In section 3 we briefly describe two recent developments of WENO schemes, namely the technique to treat negative linear weights [23] and the very high order central WENO schemes [22].

2. Finite volume and finite difference WENO schemes

A finite volume scheme for a conservation law such as (1.1) approximates an integral version of it. Let's use the one dimensional example

$$u_t + f(u)_x = 0 \tag{2.1}$$

to illustrate the ideas. Suppose $\{I_i = [x_{i-\frac{1}{2}}, x_{i+\frac{1}{2}}]\}$, $i = 1, ..., N$, is a partition of the computational domain, and $\Delta x_i = x_{i+\frac{1}{2}} - x_{i-\frac{1}{2}}$. If we integrate the PDE (2.1) in the cell I_i, we obtain

$$\frac{d\bar{u}_i(t)}{dt} + \frac{1}{\Delta x_i}\left[f(u(x_{i+\frac{1}{2}}, t)) - f(u(x_{i-\frac{1}{2}}, t))\right] = 0 \tag{2.2}$$

where

$$\bar{u}_i(t) = \frac{1}{\Delta x_i}\int_{I_i} u(x,t)dx$$

is the cell average of u in cell I_i. Notice that (2.2) is *not* a scheme yet, rather it is still an exact identity satisfied by the exact solution of the PDE (2.1). This is the starting point, though, for designing a finite volume scheme.

A semi-discrete (discrete in the spatial variable only) finite volume scheme for (2.1) is an ODE system for the cell averages $\{\bar{u}_i(t)\}$, $i = 1, ..., N$. In order to obtain such a scheme, we would need the following reconstruction procedure:

Procedure 2.1: Reconstruction. Obtain accurate point values $\{u(x_{i+\frac{1}{2}}, t)\}$, $i = 0, ..., N$, from the given cell averages $\{\bar{u}_i(t)\}$, $i = 1, ..., N$.

Notice that we have ignored possible problems at the boundary. We thus assume the data is either periodic or compactly supported. Boundary conditions can be treated in a stable and high order fashion depending on the type of boundary conditions.

WENO is simply a specific reconstruction procedure. Let us demonstrate the fifth order version. For this purpose, the approximation of $\{u(x_{i+\frac{1}{2}}, t)\}$ uses the information of five cell averages, from the stencil $\{I_{i-2}, I_{i-1}, I_i, I_{i+1}, I_{i+2}\}$. This stencil is not symmetric with respect to the point $x_{i+\frac{1}{2}}$ of the reconstruction. There is one more cell to the left than to the right. Thus this reconstruction is good for upwinding. The procedure consists of the following steps:

1. We break the final stencil

$$\mathcal{T} = \{I_{i-2}, I_{i-1}, I_i, I_{i+1}, I_{i+2}\} \tag{2.3}$$

into the following three smaller stencils:

$$\mathcal{S}_1 = \{I_{i-2}, I_{i-1}, I_i\}, \qquad \mathcal{S}_2 = \{I_{i-1}, I_i, I_{i+1}\}, \qquad \mathcal{S}_3 = \{I_i, I_{i+1}, I_{i+2}\}.$$

Notice that each small stencil contains the "target cell" I_i.

2. We construct three polynomials $p_j(x)$ of degree at most two, with their cell averages agreeing with that of the function u in the three cells in each stencil S_j. We also construct a polynomial $Q(x)$ of degree at most four, with its cell averages agreeing with that of the function u in the five cells in the larger stencil $\mathcal{T}$. The three lower order approximations to $u(x_{i+1/2})$, associated with $p_j(x)$, in terms of the given cell averages of u, are given by:

$$\begin{aligned} p_1(x_{i+1/2}) &= \frac{1}{3}\bar{u}_{i-2} - \frac{7}{6}\bar{u}_{i-1} + \frac{11}{6}\bar{u}_i, \\ p_2(x_{i+1/2}) &= -\frac{1}{6}\bar{u}_{i-1} + \frac{5}{6}\bar{u}_i + \frac{1}{3}\bar{u}_{i+1}, \\ p_3(x_{i+1/2}) &= \frac{1}{3}\bar{u}_i + \frac{5}{6}\bar{u}_{i+1} - \frac{1}{6}\bar{u}_{i+2}. \end{aligned} \tag{2.4}$$

The coefficients in front of the $\bar{u}$ could be derived by Lagrange polynomials or by solving a small 3×3 linear system, from the condition that the quadratic polynomial $p_j(x)$ has the same cell averages as the given $\bar{u}$ in the relevant stencil. See [24] for details. Each of the $p_j(x_{i+1/2})$ in (2.4) is a third order approximation to $u(x_{i+1/2})$. The fifth order approximation to $u(x_{i+1/2})$, associated with $Q(x)$, is given by:

$$Q(x_{i+1/2}) = \frac{1}{30}\bar{u}_{i-2} - \frac{13}{60}\bar{u}_{i-1} + \frac{47}{60}\bar{u}_i + \frac{9}{20}\bar{u}_{i+1} - \frac{1}{20}\bar{u}_{i+2}. \tag{2.5}$$

3. We find three constants, also called linear weights,

$$\gamma_1 = \frac{1}{10}, \qquad \gamma_2 = \frac{3}{5}, \qquad \gamma_3 = \frac{3}{10}, \tag{2.6}$$

such that

$$Q(x_{i+1/2}) = \gamma_1\, p_1(x_{i+1/2}) + \gamma_2\, p_2(x_{i+1/2}) + \gamma_3\, p_3(x_{i+1/2})$$

for all possible given data $\bar{u}_j$, $j = i-2, i-1, i, i+1, i+2$. This is to say, the higher order reconstruction $Q(x_{i+1/2})$ can be written as a linear combination of three lower order reconstructions $p_j(x_{i+1/2})$. The linear weights given in (2.6) depend on local geometry and order of accuracy, but not on $\bar{u}_j$. If some of these linear weights are negative, special techniques must be used and will be described in next section.

4. We compute the smoothness indicator, denoted by β_j, for each stencil S_j, which measures how smooth the function $p_j(x)$ is in the target cell I_j. The smaller this smoothness indicator β_j, the smoother the function $p_j(x)$ is in the target cell. In most of the currently used WENO schemes the following smoothness indicator [11] is used:

$$\beta_j = \sum_{l=1}^{2} \int_{I_i} \Delta x^{2l-1} \left(\frac{d^l}{dx^l} p_j(x) \right)^2 dx \tag{2.7}$$

for $j = 1, 2, 3$, for this fifth order case. These smoothness indicators are quadratic functions of the cell averages in the stencil. For this fifth order case they can be worked out as follows:

$$\begin{aligned}
\beta_1 &= \frac{13}{12}\left(\bar{u}_{i-2} - 2\bar{u}_{i-1} + \bar{u}_i\right)^2 + \frac{1}{4}\left(\bar{u}_{i-2} - 4\bar{u}_{i-1} + 3\bar{u}_i\right)^2 \\
\beta_2 &= \frac{13}{12}\left(\bar{u}_{i-1} - 2\bar{u}_i + \bar{u}_{i+1}\right)^2 + \frac{1}{4}\left(\bar{u}_{i-1} - \bar{u}_{i+1}\right)^2 \qquad (2.8) \\
\beta_3 &= \frac{13}{12}\left(\bar{u}_i - 2\bar{u}_{i+1} + \bar{u}_{i+2}\right)^2 + \frac{1}{4}\left(3\bar{u}_i - 4\bar{u}_{i+1} + \bar{u}_{i+2}\right)^2
\end{aligned}$$

5. We compute the nonlinear weights based on the smoothness indicators:

$$\omega_j = \frac{\tilde{\omega}_j}{\sum_l \tilde{\omega}_l}, \qquad \tilde{\omega}_j = \frac{\gamma_j}{(\varepsilon + \beta_j)^2} \qquad (2.9)$$

where γ_j are the linear weights determined in step 3 above, and ε is a small number to avoid the denominator to become 0. Typically, we can take $\varepsilon = 10^{-6}$ in all the computations. The final WENO approximation or reconstruction is then given by

$$R(x_{i+1/2}) = \omega_1\ p_1(x_{i+1/2}) + \omega_2\ p_2(x_{i+1/2}) + \omega_3\ p_3(x_{i+1/2}) \qquad (2.10)$$

With this WENO reconstruction procedure, a finite volume WENO scheme is now ready. We give here a very brief summary of all the steps of a WENO finite volume scheme applied to (2.1) in the one dimensional scalar case for the positive wind $f'(u) \geq 0$. More details can be found in, e.g., [11, 24, 25]. The algorithm consists of the following steps:

1. Given the cell averages $\bar{u}_i$ for all cells I_i for time level n (starting from time level 0 which is the initial condition);
2. Reconstruct the point values $u^-_{i+1/2}$ for all cell boundaries $x_{i+1/2}$ using the reconstruction procedure detailed above. That is, we use (2.10) with ω_j defined by (2.9), using γ_j given by (2.6) and β_j given by (2.8). The superscript "$-$" in $u^-_{i+1/2}$ refers to the fact that the reconstruction has a stencil (2.3) biased to the left relative to the location $x_{i+1/2}$. This is upwinding according to the wind direction $f'(u) \geq 0$.
3. Form the residue for time level n in the method-of-lines ODE

$$\frac{d\bar{u}_i}{dt} = \frac{1}{\Delta x}\left(f(u^-_{i+1/2}) - f(u^-_{i-1/2})\right),$$

and move to time level $n+1$ by a high order TVD Runge-Kutta method [26].

Next we describe the setup of a finite difference scheme for solving (2.1). A semi-discrete finite difference scheme for (2.1) is an ODE system for the point values $\{u_i(t)\}$, $i = 1, ..., N$, where $u_i(t)$ approximate the point values of the solution $u(x_i, t)$. We also insist on a *conservative* approximation to the derivative $f(u)_x$ in the form of

$$f(u)_x|_{x=x_i} \approx \frac{1}{\Delta x}\left(\hat{f}_{i+1/2} - \hat{f}_{i-1/2}\right) \tag{2.11}$$

where $\hat{f}_{i+1/2}$ is the numerical flux, which typically is a Lipschitz continuous function of several neighboring values of u_j around x_i.

At a first glance, the finite difference scheme has nothing in common with the finite volume scheme described above, as they approximate different values of the solution. However, the following observation, first introduced in [27], establishes a close relationship between the two. If we identify a function $h(x)$ by

$$f(u(x)) = \frac{1}{\Delta x}\int_{x-\frac{\Delta x}{2}}^{x+\frac{\Delta x}{2}} h(\xi)d\xi, \tag{2.12}$$

where we have suppressed the t dependency of the function as we are interested now only at spatial discretizations, then by just taking derivatives on both sides of the above equality we obtain

$$f(u(x))_x = \frac{1}{\Delta x}\left[h\left(x + \frac{\Delta x}{2}\right) - h\left(x - \frac{\Delta x}{2}\right)\right].$$

This means that we only need to take the numerical flux as

$$\hat{f}_{i+1/2} = h(x_{i+1/2}). \tag{2.13}$$

If we could get an approximation to $h(x)$ to high order accuracy, the conservative approximation to the derivative in (2.11) would also be of the same high order of accuracy. Notice that (2.12) can be written as

$$f(u_i) = \bar{h}_i,$$

i.e. we are given the cell averages of h (since we know the point values u_i, hence also $f(u_i)$, in a finite difference scheme) and we would need to reconstruct its point values $h(x_{i+1/2})$ for the numerical flux (2.13). But this is *exactly the same* reconstruction problem in Procedure 2.1 above for finite volume schemes!

Thus for one space dimension, the finite difference and finite volume schemes share the same reconstruction procedure, applied in different contexts (on cell averages of u for the finite volume schemes, and on point

values of $f(u)$ for the finite difference schemes). They involve the same complexity and cost. Finite difference schemes are more restrictive in the situations that they can be applied, as they only work for uniform or smooth varying meshes and a flux splitting (for upwinding) must be smooth.

However, for multiple space dimensions, there are essential differences between these two classes of methods, when the order of accuracy is at least three. While finite difference schemes can still be applied in a dimension-by-dimension fashion (*not* dimension splitting!), i.e. computing $f(u)_x$ along a x-line with fixed y using the procedure above, and likewise for $g(u)_y$, then adding them together to form the residue, finite volume schemes of third order or higher must involve multi-dimensional reconstructions from cell averages to point values and then numerical integrations to get the numerical fluxes along the boundaries of cells. The details of these reconstructions can be found in, e.g., [24, 25, 9, 23]. As such, the operation count and CPU time for a finite volume scheme is around two to four times more expensive in two dimensions and around five to nine times more expensive in three dimensions, compared with a finite difference scheme of the same order of accuracy, see, e.g. [3] for such a comparison for ENO schemes. In return, the finite volume schemes do allow more flexibility in their applications. They can be applied in arbitrary triangulations and do not require smoothness of the meshes. On the other hand, finite difference schemes can only be applied to uniform rectangular or smooth curvilinear coordinates.

3. Two recent developments of WENO schemes

In this section we briefly describe two recent developments in WENO schemes. The first is a technique to treat negative linear weights in [23]. The second is a class of high order central WENO schemes in [22].

3.1. A TECHNIQUE TO TREAT NEGATIVE LINEAR WEIGHTS

As we can see from the previous section, a key idea in the WENO reconstruction is to write a high order reconstruction as a linear combination of several lower order reconstructions. The combination coefficients, also called linear weights, are determined by local geometry and order of accuracy. In many cases these linear weights are positive, such as in (2.6). However there are also situations where some of them become negative. For example, if we have exactly the same setting as in the previous section but now we seek the reconstruction not at the cell boundary but at the cell center x_i, as needed by the central schemes with staggered grids [13], [22], then step 1 would stay the same as above; step 2 would produce

$$p_1(x_i) = -\frac{1}{24}\bar{u}_{i-2} + \frac{1}{12}\bar{u}_{i-1} + \frac{23}{24}\bar{u}_i,$$

$$p_2(x_i) = -\frac{1}{24}\bar{u}_{i-1} + \frac{13}{12}\bar{u}_i - \frac{1}{24}\bar{u}_{i+1}, \tag{3.1}$$
$$p_3(x_i) = \frac{23}{24}\bar{u}_i + \frac{1}{12}\bar{u}_{i+1} - \frac{1}{24}\bar{u}_{i+2}.$$

Each of them is a third order reconstruction to $u(x_i)$. The fifth order reconstruction to $u(x_i)$, associated with $Q(x)$, is given by:

$$Q(x_i) = \frac{3}{640}\bar{u}_{i-2} - \frac{29}{480}\bar{u}_{i-1} + \frac{1067}{960}\bar{u}_i - \frac{29}{480}\bar{u}_{i+1} + \frac{3}{640}\bar{u}_{i+2}. \tag{3.2}$$

Step 3 would produce the following weights:

$$\gamma_1 = -\frac{9}{80}, \qquad \gamma_2 = \frac{49}{40}, \qquad \gamma_3 = -\frac{9}{80}.$$

Notice that two of them are negative. The smoothness indicators in step 4 will remain the same. This time, the WENO approximation, when naively applied, leads to unstable results because of the negative linear weights. As an example, in Fig. 3.1, left, we show the results of using a fourth order finite volume WENO scheme [9] on a non-uniform triangular mesh, for solving the two dimensional Burgers equation:

$$u_t + \left(\frac{u^2}{2}\right)_x + \left(\frac{u^2}{2}\right)_y = 0 \tag{3.3}$$

in the domain $[-2,2] \times [-2,2]$ with an initial condition $u_0(x,y) = 0.3 + 0.7 \sin\left(\frac{\pi}{2}(x+y)\right)$ and periodic boundary conditions. We can see that serious oscillation appears near the shock in the numerical solution once the shock has developed. The oscillation eventually leads to instability and blowing up of the numerical solution for this example.

A simple splitting technique of treating negative weights in WENO schemes is developed by Shi, Hu and Shu in [23]: we first split the linear weights into two groups

$$\tilde{\gamma}_i^+ = \frac{1}{2}\left(\gamma_i + 3\left|\gamma_i\right|\right), \qquad \tilde{\gamma}_i^- = \tilde{\gamma}_i^+ - \gamma_i, \qquad i = 1,2,3$$

and scale them by

$$\sigma^{\pm} = \sum_{j=1}^{3} \tilde{\gamma}_j^{\pm}; \qquad \gamma_i^{\pm} = \tilde{\gamma}_i^{\pm}/\sigma^{\pm}, \qquad i = 1,2,3.$$

For the simple example of fifth order WENO reconstruction to $u(x_i)$, the split linear weights are, before the scaling,

$$\tilde{\gamma}_1^+ = \frac{9}{80}, \ \tilde{\gamma}_1^- = \frac{9}{40}, \qquad \tilde{\gamma}_2^+ = \frac{49}{20}, \ \tilde{\gamma}_2^- = \frac{49}{40}, \qquad \tilde{\gamma}_3^+ = \frac{9}{80}, \ \tilde{\gamma}_3^- = \frac{9}{40}.$$

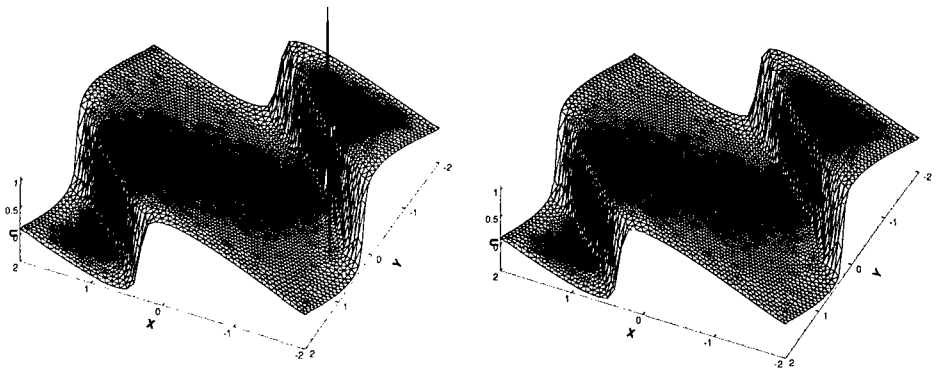

Figure 3.1. 2D Burgers' equation. Left: fourth order WENO result at $t = 0.473$, CFL=0.2, without any special treatment for the negative linear weights; Right: fourth order WENO solution at $t = 5/\pi^2$, CFL=0.2, with the treatment for the negative linear weights.

The WENO reconstruction is now performed on each group separately, by computing the nonlinear weights (2.9) separately for $\omega_j^{\pm}$ with the same smoothness indicators β_j in (2.7). The final WENO reconstruction is then taken as σ^+ times the reconstruction using the group of positive weights minus σ^- times the reconstruction using the group of negative weights. The key idea of this decomposition is to make sure that every stencil has a significant representation in both the positive and the negative weight groups. Within each group, the WENO idea of redistributing the weights subject to a fixed sum according to the smoothness of the approximation is still followed as before. For more details, we refer to [23].

We notice that, as the most expensive part of the WENO procedure, namely the computation of the smoothness indicators (2.7), has not changed, the extra cost of this positive/negative weight splitting is very small. However this simple and inexpensive change makes a big difference to the computations. In Fig. 3.1, right, we show the result of the approximation to the Burgers equation, now using WENO schemes with this splitting treatment. We can see clearly that the results are now as good as one would get from WENO schemes having only positive linear weights.

3.2. HIGH ORDER CENTRAL WENO SCHEMES

In [22] a class of fourth and eighth order central WENO (CWENO) schemes have been constructed and the role of local characteristic decompositions on eliminating spurious oscillations is demonstrated. We will give a brief description of such schemes here.

The notations are the same as before, plus the new one for staggered cells $I_{i+\frac{1}{2}} = [x_i, x_{i+1}]$. Let Δt be the time step, $u_i^n = u(x_i, t^n)$ denotes the point values, and $\overline{u}_i^n = \frac{1}{\Delta x}\int_{I_i} u(x,t^n)dx$, $\overline{u}_{i+\frac{1}{2}}^n = \frac{1}{\Delta x}\int_{I_{i+\frac{1}{2}}} u(x,t^n)dx$ represent the cell averages at time t^n on the cells I_i and $I_{i+\frac{1}{2}}$, respectively. The CWENO scheme approximates the cell averages at time t^{n+1} based on their values at time t^n with staggered space grids. We integrate (2.1) over the region $I_{i+\frac{1}{2}} \times [t^n, t^{n+1}]$, to get an equivalent formulation:

$$\overline{u}_{i+\frac{1}{2}}^{n+1} = \overline{u}_{i+\frac{1}{2}}^n - \frac{1}{\Delta x}\left[\int_{t^n}^{t^{n+1}} f(u(x_{i+1},t))dt - \int_{t^n}^{t^{n+1}} f(u(x_i,t))dt\right] \tag{3.4}$$

What we want to do is to find approximations of the cell averages $\overline{u}_{i+\frac{1}{2}}^n$ and the two integrals in (3.4). Thus the algorithm consists of two major steps to evolve from $\{\overline{u}_i^n\}$ to $\{\overline{u}_{i+\frac{1}{2}}^n\}$:

1. The approximation of $\overline{u}_{i+\frac{1}{2}}^n$ from the knowledge of $\{\overline{u}_i^n\}$ by a WENO reconstruction. Notice that

$$\overline{u}_{i+\frac{1}{2}}^n = \frac{1}{\Delta x}\int_{x_i}^{x_{i+1}} u(x,t^n)dx = \frac{1}{\Delta x}\left[\int_{x_i}^{x_{i+\frac{1}{2}}} u(x,t^n)dx + \int_{x_{i+\frac{1}{2}}}^{x_{i+1}} u(x,t^n)dx\right],$$

   hence we only need to reconstruct $\frac{1}{\Delta x}\int_{x_{i-\frac{1}{2}}}^{x_i} u(x,t^n)dx$ for all i because

$$\frac{1}{\Delta x}\int_{x_i}^{x_{i+\frac{1}{2}}} u(x,t^n)dx = \overline{u}_i^n - \frac{1}{\Delta x}\int_{x_{i-\frac{1}{2}}}^{x_i} u(x,t^n)dx \tag{3.5}$$

   by conservation. The WENO reconstruction for this step is very similar to Procedure 2.1.
2. The approximation of $\int_{t^n}^{t^{n+1}} f(u(x_i,t))dt$. If the time step Δt is subject to a restrictive CFL condition $\Delta t \le \frac{\Delta x}{2}\max|f'(u)|$, we can assume that $u(x_i,t)$ is smooth, since the discontinuities starting at t^n from the staggered grid points $x_{i-\frac{1}{2}}$ and $x_{i+\frac{1}{2}}$ have not reached the cell boundary x_i yet. Hence no Riemann solvers are needed and the time integrals can be evaluated with a quadrature formula to high order accuracy. Notice that this is equivalent to a Lax-Friedrichs scheme and the same effect can also be achieved without a staggered mesh by just using a Lax-Friedrichs building block, such as those WENO finite difference schemes in [11], [1] where the Lax-Friedrichs building blocks are used and no Riemann solvers are needed either. We could for example use

a three point Gauss quadrature, obtaining

$$\int_{t^n}^{t^{n+1}} f(u(x_i,t))dt \approx \Delta t \sum_{l=1}^{3} \alpha_l f(u(x_i, t^n + \Delta t \tau_l))$$

where α_l and τ_l are the weights and knots of the Gauss quadrature, respectively. Now what we want to do is to find the approximation of the point values $u(x_i, t^n + \Delta t\tau_l)$ from the cell averages $\{\overline{\mu}^n\}$. This can be achieved by solving the ODE at the grid points $x = x_i$:

$$\begin{cases} \frac{du(x_i,t)}{dt} = -(f(u))_x|_{x_i} \\ u(x_i, t^n) \approx \mu^n \end{cases} \tag{3.6}$$

with μ^n computed by a WENO reconstruction from the cell averages $\{\overline{\mu}^n\}$, very similar to Procedure 2.1 above. The ODE (3.6) is solved by a Runge-Kutta method to obtain the approximation of $u(x_i, t^n + \Delta t\tau_l)$, with the aid of natural continuous extension (NCE) for (3.6), [29], see [2] and [22] for details.

Acknowledgment: The author's research has been partially supported by ARO grant DAAD19-00-1-0405, NSF grants DMS-9804985 and ECS-9906606, and AFOSR grant F49620-99-1-0077.

References

1. D. Balsara and C.-W. Shu, *Monotonicity preserving weighted essentially non-oscillatory schemes with increasingly high order of accuracy*, J. Comput. Phys., v160 (2000), pp.405-452.
2. F. Bianco, G. Puppo and G. Russo, *High-order central schemes for hyperbolic systems of conservation laws*, SIAM J. Sci. Comput., v21 (1999), pp.294-322.
3. J. Casper, C.-W. Shu and H.L. Atkins, *Comparison of two formulations for high-order accurate essentially nonoscillatory schemes*, AIAA J., v32 (1994), pp.1970-1977.
4. L. Del Zanna, M. Velli and P. Londrillo, *Dynamical response of a stellar atmosphere to pressure perturbations: numerical simulations*, Astron. Astrophys., v330 (1998), pp.L13-L16.
5. O. Friedrichs, *Weighted essentially non-oscillatory schemes for the interpolation of mean values on unstructured grids*, J. Comput. Phys., v144 (1998), pp.194–212.
6. F. Grasso and S. Pirozzoli, *Shock-wave-vortex interactions: Shock and vortex deformations, and sound production*, Theor. Comp. Fluid Dyn., v13 (2000), pp.421-456.
7. F. Grasso and S. Pirozzoli, *Shock wave-thermal inhomogeneity interactions: Analysis and numerical simulations of sound generation*, Phys. Fluids, v12 (2000), pp.205-219.
8. A. Harten, B. Engquist, S. Osher and S. Chakravarthy, *Uniformly high order essentially non-oscillatory schemes, III*, J. Comput. Phys., v71 (1987), pp.231–303.
9. C. Hu and C.-W. Shu, *Weighted Essentially Non-Oscillatory Schemes on Triangular Meshes*, J. Comput. Phys., v150 (1999), pp.97-127.
10. G. Jiang and D.-P. Peng, *Weighted ENO schemes for Hamilton-Jacobi equations*, SIAM J. Sci. Comput., v21 (2000), pp.2126-2143.

11. G. Jiang and C.-W. Shu, *Efficient implementation of weighted ENO schemes*, J. Comput. Phys., v126 (1996), pp.202–228.
12. G. Jiang and C.-C. Wu, *A high order WENO finite difference scheme for the equations of ideal magnetohydrodynamics*, J. Comput. Phys., v150 (1999), pp.561-594.
13. D. Levy, G. Puppo and G. Russo, *Central WENO schemes for hyperbolic systems of conservation laws*, Math. Model. Numer. Anal. (M^2AN), v33 (1999), pp.547-571.
14. D. Levy, G. Puppo and G. Russo, *Compact central WENO schemes for multidimensional conservation laws*, SIAM J. Sci. Comput., v22 (2000), pp.656-672.
15. D. Levy, G. Puppo and G. Russo, *A third order central WENO scheme for 2D conservation laws*, Appl. Numer. Math. v33 (2000),415–421.
16. S. Liang and H. Chen, *Numerical simulation of underwater blast-wave focusing using a high-order scheme*, AIAA J., v37 (1999), pp.1010-1013.
17. R. Liska and B. Wendroff, *Composite schemes for conservation laws*, SIAM J. Numer. Anal., v35 (1998), pp.2250-2271.
18. R. Liska and B. Wendroff, *Two-dimensional shallow water equations by composite schemes*, Int. J. Numer. Meth. Fl., v30 (1999), pp.461-479.
19. X.-D. Liu, S. Osher and T. Chan, *Weighted essentially non-oscillatory schemes*, J. Comput. Phys., v115 (1994), pp.200–212.
20. P. Montarnal and C.-W. Shu, *Real gas computation using an energy relaxation method and high order WENO schemes*, J. Comput. Phys., v148 (1999), pp.59-80.
21. S. Noelle, *The MoT-ICE: a new high-resolution wave-propagation algorithm for multidimensional systems of conservation laws based on Fey's method of transport*, J. Comput. Phys., v164 (2000), pp.283-334.
22. J. Qiu and C.-W. Shu, *On the construction, comparison, and local characteristic decomposition for high order central WENO schemes*, J. Comput. Phys., submitted.
23. J. Shi, C. Hu and C.-W. Shu, *A technique of treating negative weights in WENO schemes*, J. Comput. Phys., to appear.
24. C.-W. Shu, *Essentially non-oscillatory and weighted essentially non-oscillatory schemes for hyperbolic conservation laws*, in *Advanced Numerical Approximation of Nonlinear Hyperbolic Equations*, B. Cockburn, C. Johnson, C.-W. Shu and E. Tadmor (Editor: A. Quarteroni), Lecture Notes in Mathematics, volume 1697, Springer, 1998, pp.325-432.
25. C.-W. Shu, *High order ENO and WENO schemes for computational fluid dynamics*, in *High-Order Methods for Computational Physics*, T.J. Barth and H. Deconinck, editors, Lecture Notes in Computational Science and Engineering, volume 9, Springer, 1999, pp.439-582.
26. C.-W. Shu and S. Osher, *Efficient implementation of essentially non-oscillatory shock capturing schemes*, J. Comput. Phys., v77 (1988), pp.439-471.
27. C.-W. Shu and S. Osher, *Efficient implementation of essentially non-oscillatory shock capturing schemes, II*, J. Comput. Phys., v83 (1989), pp.32-78.
28. J. Yang, S. Yang, Y. Chen and C. Hsu, *Implicit weighted ENO schemes for the three-dimensional incompressible Navier-Stokes equations*, J. Comput. Phys., v146 (1998), pp.464-487.
29. M. Zennaro, *Natural continuous extensions of Runge-Kutta methods*, Math. Comp., v46 (1986), pp.119-133.